

Investigation of Stray Losses in Converter Transformer Using Parametric Analysis of Wall Shunt Thickness

J.U. Kothavade*, P. Kundu

Department of Electrical Engineering, SVNIT, Surat, Gujarat, India

Abstract— In High Voltage Direct Current Transmission (HVDC) system, converter transformer is an integral part of the system. Generally, core loss, copper loss and stray losses occur in the transformer. In which stray losses are produced in the transformers metallic parts such as transformer tank which can be 10% to 15% of the total loss. Experimentally, stray losses are difficult to measure. So, it is essential to use numerical modelling to predict the stray loss. The secondary winding of the converter transformer is directly linked to the rectifier or inverter. As a result, the converter transformer winding's current is non-sinusoidal. Due to non-sinusoidal current, losses are more in converter transformer than in the power transformer. This article analyses the stray loss reduction techniques by applying wall shunt on the transformer tank surface. These stray losses are estimated for different wall shunt thickness values by varying the thickness of wall shunt using parametric analysis in 3-D finite-element analysis (FEA). Two types of wall shunts is used:-horizontal and vertical. In which horizontal wall shunt results are compared with the vertical wall shunt for non-sinusoidal and sinusoidal current excitation, where sinusoidal excitation is a fundamental component of non-sinusoidal excitation. For a case study, 315 MVA converter transformer is used to estimate stray losses on this transformer. The results obtained by the numerical method are also compared with the analytical method. Result shows that the stray losses are decreased with an increase in wall shunt thickness. Also, these losses are less for sinusoidal excitation than the non-sinusoidal excitation.

Keywords—Parametric Analysis, Converter Transformer, stray loss, non-sinusoidal excitation, horizontal wall shunt, sinusoidal excitation, vertical wall shunt.

1. INTRODUCTION

Nowadays, power demand is continuously increasing with a slight increase in power generation. Low loss power transmission system meets the power demand [1–3]. So, High Voltage Direct Current Transmission (HVDC) system is used for long-distance power transmission as it has low power transmission losses. This transmission system uses a direct current (DC) supply for the power transmission. In HVDC system, two alternating current (AC) stations of different frequencies are connected through an HVDC link [4]. A generating system, converter transformer, rectifier and inverter station is the essential components of the HVDC system.

Converter transformer is the essential component of the HVDC system and it is connected between AC system and rectifier or inverter station. Also, it acts as a galvanic separation between AC and DC system. Core loss, copper loss and stray loss are the main losses developed in the transformer [5–8]. In which stray losses are produced due to leakage field links with the metallic parts of the transformer i.e. transformer tank [9–12]. These stray losses are 10% to 15% of the total losses. To reduce these stray losses in the transformer magnetic wall shunt is applied to the transformer tank. This magnetic wall shunt provides a low reluctance path for the leakage fluxes; so a small number of leakage fluxes interact with the transformer tank [13–16]. The secondary winding of the converter transformer is directly linked to the rectifier or inverter. Due to the sequence operation of diodes in the rectifier, the current

flowing through the converter transformer is non-sinusoidal. Losses in converter transformer are more than the normal transformer due to non-sinusoidal current. In a real transformer, stray loss calculation is difficult, and assessment requires more time and effort. So, numerical analysis is used for the calculation of stray loss [17, 18]. In ANSYS MAXWELL 3D simulation, the 3D finite element analysis (FEA) approach is used for numerical analysis.

Transformers core, tank and windings design steps are discussed in [19] and [20]. HVDC transmission systems necessity and limitations; three-phase and single-phase rectifier working studied in [21]. The detailed description of rating, insulation design and different configurations of converter transformer is explained in [22]. In [23] discussed the root causes of stray loss generation and the effect of these losses on the winding of transformer. During short circuit conditions, leakage fluxes are increased, which causes an increase in electromagnetic forces, so the effect of these forces on converter transformer is discussed in [24]. In power transformer, leakage fluxes produced due to interturn faults and the effect of these fluxes on the transformer winding is discussed in [15]. In [25] analyses the impact of lobe type magnetic shielding on leakage fluxes and stray losses for 334MVA single-phase auto-transformer. These stray losses are analysed by the 3D finite-element method (FEM) method. In [26] discussed the effects of losses and leakage reactance for distribution transformer on powers systems grid reliability and stability. Also, these losses are estimated by the analytical method and numerical method as well as using FEM method. In [27] discusses the different methods for optimal location of wall shunt on distribution power transformer. In [28, 29], several structures of magnetic shunts in power transformers are investigated using the FEM. In [30] analysed the leakage flux distribution on 200kVA power transformer. Also, stray losses are calculated for different materials of wall shunt in which magnetic shielding gives effectively reduced stray losses as compare to copper shielding. In [31] discussed the effect of change

Received: 18 Oct. 2021

Revised: 23 Aug. 2022

Accepted: 07 Oct. 2022

* Corresponding author:

E-mail: jayesh.kothavade@gmail.com (J. Kothavade)

DOI: 10.22098/JOAPE.2022.9696.1676

Research Paper

©2023 University of Mohaghegh Ardabili. All rights reserved

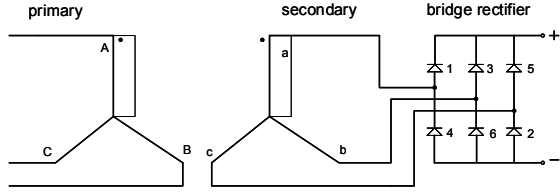


Fig. 1. Bridge Connection

in vertical wall thickness on stray loss for power transformer. Vertical and horizontal shunt comparisons and the influence of magnetic wall shunts are explained in [32, 33].

In this paper, converter transformer's stray losses are reduced by the wall shunt applied to the transformer tank. Vertical and horizontal wall shunts are the two types of wall shunts used. Horizontal wall shunt configuration compares to the vertical wall shunt configuration in converter transformer. Parametric analysis of wall shunt thickness is analysed, i.e. thickness of wall shunt is varied and stray losses evaluated. The novelty of this paper is stray losses are analysed for both types of wall shunt applying non-sinusoidal and sinusoidal current excitation in which sinusoidal excitation is a fundamental component of the non-sinusoidal excitation. This stray loss is analysed on three winding converter transformer. In parametric analysis of wall shunt thickness, Stray losses are calculated using 3D FEA method in ANSYS MAXWELL. Stray losses calculated using 3D FEA method are also compared with the analytical method.

2. THEORY

2.1. Converter Transformer Bridge Connection

The AC supply excites the primary winding of the converter transformer, and the secondary winding terminals are linked directly to the bridge rectifier, as illustrated in Fig. 1. Single two-winding transformer is used for 6 pulse rectifiers, and 2 two-winding transformers are used for 12 pulse rectifiers, one of which is star-star and the other is star-delta combination; alternatively, one three-winding transformer can be used [22]. Fig. 2 depicts the transformer's winding current and the diode's sequence operation. Each diode will operate for 120° .

Equation (2) gives the root mean square (RMS) value of the fundamental component of the waveform illustrated in Fig. 2 using Fourier analysis [19, 21].

$$\sqrt{2} I_{L1} = \frac{2}{\pi} \int_{-\pi/3}^{\pi/3} I_d \cos \theta d\theta = \frac{2}{\pi} I_d [\sin \theta]_{-\pi/3}^{\pi/3} = \frac{2\sqrt{3}}{\pi} I_d = 1.11 I_d \quad (1)$$

The fundamental current's RMS value is

$$I_{L1} = \frac{\sqrt{6}}{\pi} I_d = 0.78 I_d \quad (2)$$

2.2. Stray Loss

Eddy current, created by leakage flux in the transformer winding, causes power loss in the transformer tank. Stray loss is the power loss in the transformer tank that can be estimated using the Poynting vector. Maxwell's equations are used to compute the stray loss [22, 31, 34].

$$\nabla \times \vec{E} = -\frac{\partial \vec{B}}{\partial t} \quad (3)$$

$$\nabla \times \vec{H} = \vec{J} \quad (4)$$

$$\nabla \cdot \vec{B} = 0 \quad (5)$$

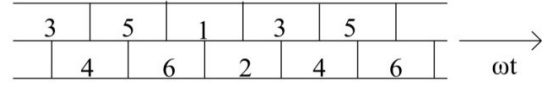


Fig. 2. Diode's Sequence Operation and Current of Secondary Winding

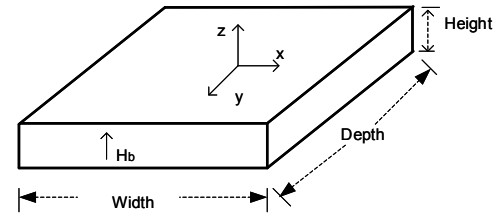


Fig. 3. Structural Component of Stray Loss

Two constitutive equations are

$$\vec{B} = \mu \vec{H} \quad (6)$$

$$\vec{J} = \sigma \vec{E} \quad (7)$$

Where, \vec{B} = flux density (Wb/m^2), σ = conductivity (mhos/m), \vec{H} = magnetic field strength (A/m), \vec{J} = current density (A/m^2), \vec{E} = electric field strength (V/m), μ = permeability of material (H/m), Apply curl to equation (4) on both sides and use vector algebra to simplify it.

$$\nabla(\nabla \cdot \vec{H}) - \nabla^2 \vec{H} = \nabla \times \vec{J} \quad (8)$$

Equation (8) is written as using equations (3), (5), (6), and (7).

$$\nabla^2 \vec{H} - \sigma \mu \frac{\partial \vec{H}}{\partial t} = 0 \quad (9)$$

Consider structural component, as illustrated in Fig. 3. The current density (J_x) and the magnetic field intensity (H_y) are believed to be components of z . Rewrite the equation (9) using complex permeability as shown below:

$$\frac{d^2 H_y}{dz^2} = j\omega\mu\sigma H_y \quad (10)$$

$$\begin{aligned} \text{When } z = 0 \quad H_y &= H_b; \\ \text{When } z = \infty \quad H_y &= 0. \end{aligned}$$

Equation (10) can be simplified by using the aforementioned condition.

$$H_y = H_b e^{-nz} \quad (11)$$

$$n = \sqrt{j\omega\mu\sigma} = (1+j) \sqrt{\frac{\omega\mu\sigma}{2}} \quad (12)$$

Where, H_b = constant, n = propagation constant. Simplify equation (11) and (12),

$$H_y = H_b e^{-\frac{(1+j)z}{\delta}} \quad (13)$$

Simplify equation (4) and (13) using vector algebra,

$$J_x = \frac{(1+j)}{\delta} H_b e^{-\frac{(1+j)z}{\delta}} \quad (14)$$

Table 1. Converter transformers specification

Classification	Value
MVA rating	315MVA, 1 \emptyset , 3 winding
Valve winding Voltage (LV)	$\frac{213}{\sqrt{3}}$ kV star and 213kV delta
Line Winding Voltage (HV)	$\frac{400}{\sqrt{3}}$ kV

Table 2. Dimensions of converter transformer

Quantity	Value	Unit
Low Voltage (LV) Winding Voltage	$\frac{213}{\sqrt{3}}$	kV
Medium Voltage (MV) Winding Voltage	213	kV
High Voltage (HV) Winding Voltage	$\frac{400}{\sqrt{3}}$	kV
LV Winding Turns	274	-
MV Winding Turns	474	-
HV Winding Turns	515	-
Width of Window	2361.98	mm
Height of Window	4945.21	mm
Height of LV Winding	4803	mm
Height of MV Winding	4721	mm
Height of HV Winding	4709	mm
Inside Diameter of LV Winding	1429.5	mm
Inside Diameter of MV Winding	1610	mm
Inside Diameter of HV Winding	1772	mm
Tank Dimension	6030.38 x 2352 x 8120	mm
Plates of Vertical Wall Shunt	380 x m x 4820	mm
Plates of Horizontal Wall Shunt	5600 x m x 380	mm

Transformer tanks time average density of stray loss can be evaluated by real part of complex poynting vector at the surface.

$$P = \frac{1}{2} \text{Re}[E \times H^*] \quad (15)$$

Simplifying equation (13), (14) and (15) on the surface at z=0. The stray loss per unit surface area is,

$$P = \frac{1}{2} \text{Re}\left[\frac{(1+j)}{\sigma} \frac{H_b^2}{\delta}\right]$$

$$\therefore P = \frac{1}{2} \frac{H_b^2}{\delta \sigma}$$

$$P = \sqrt{\frac{\omega \mu}{2\sigma}} \frac{H_b^2}{2}$$

Therefore, the total power loss of the transformer tank is,

$$P = \sqrt{\frac{\omega \mu}{8\sigma}} \int_{\text{surface}} H_b^2 ds \quad (17)$$

3. SYSTEM DEVELOPMENT

In this paper, converter transformer is designed and the specifications taken from the Rihand HVDC station. Converter transformer specifications are illustrated in Table 1 [23].

Fig. 5 shows the converter transformer with a horizontal wall shunt. In horizontal wall shunt, wall shunt placed parallel to the yoke and near to the transformer tank. There are 6 horizontal plates applied on the front side and 6 on the backside of converter transformer. Also, transformers right and left side include 4 vertical plates each. In horizontal wall shunt, 8 vertical plates and 12 horizontal plates are used. Dimensions of each plate shown in Table 2.

Fig. 6 shows the converter transformer with a vertical wall shunt. In vertical wall shunt, wall shunt placed in parallel to the HV winding. There are 10 vertical plates on the front side and 10 on the backside of converter transformer. Also, transformers right and left side include 5 vertical plates each. In vertical wall shunt, 30 vertical plates are used. Dimensions of each plate illustrated in Table 2. Where m denoted as the thickness of wall shunt. In this paper, stray losses are analysed by parametric analysis of wall

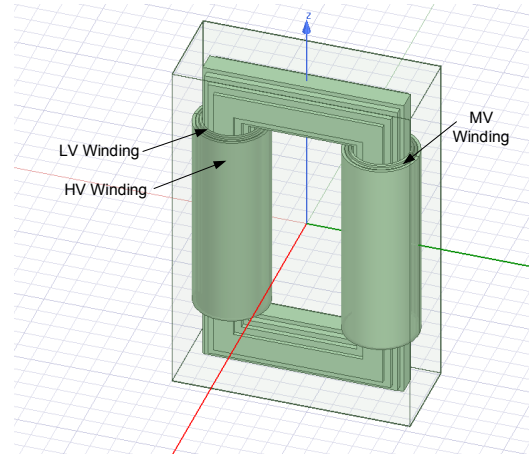


Fig. 4. Designed Converter Transformer

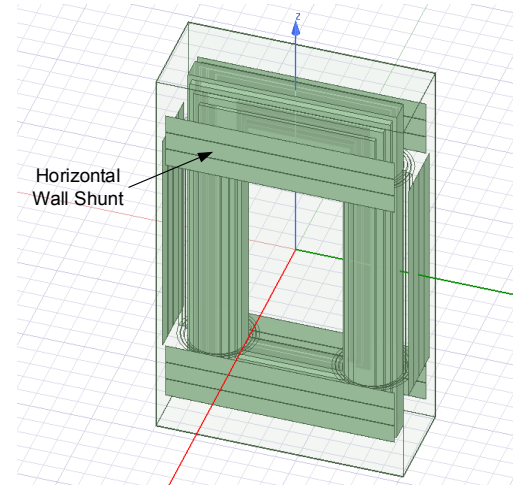


Fig. 5. Designed Converter Transformer With Horizontal Wall Shunt

shunt thickness. For parametric analysis, wall shunt thickness is varied from 4mm to 40mm with a step of 2mm and stray losses calculated at each wall shunt thickness. If the wall shunt thickness is 40mm, the minimum clearance between the wall shunt and the outside surface of HV winding is i) length side 100mm ii) breadth side 150mm.

JFE Steel 35, M5, copper, and steel 1008 are the materials used for the core, wall shunt, winding, and tank, respectively, in the designing of converter transformer. Current flowing through the converter transformer is non-sinusoidal; so, for the simulation of converter transformer two cases are considered i) sinusoidal excitation ii) non-sinusoidal excitation. Sinusoidal excitation's rms value is determined from equation (2).

4. RESULTS AND DISCUSSION

In this section, stray losses of the designed converter transformer are calculated by simulating the converter transformer in ANSYS-MAXWELL software. These stray losses are computed by parametric analysis of wall shunt thickness at full load condition. Converter transformer's LV winding is excited by the rated current for simulation, whereas MV and HV winding is applied by the resistive load. For the current excitation, two significant cases are considered i) sinusoidal current excitation ii) non-sinusoidal current excitation. Sinusoidal current excitation is the fundamental component of non-sinusoidal current excitation. Stray losses are

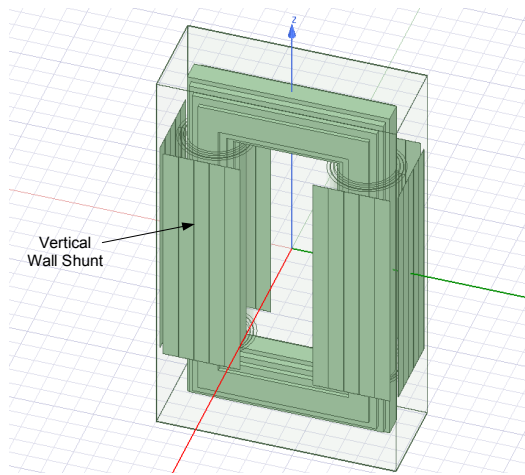


Fig. 6. Designed Converter Transformer with Vertical Wall Shunt

calculated for vertical as well as horizontal wall shunt for both excitations. Fig. 7 shows the flow diagram for calculating stray losses in converter transformer using the 3D FEA method. The meshed model for the designed converter transformer shown in Fig. 8 and Fig. 9 respectively.

4.1. Vertical Wall Shunt

In this case, to reduce stray losses vertical wall shunt is used, which is placed parallel to the outer winding, as shown in Fig. 6.

A) Sinusoidal Excitation

LV winding of the converter transformer is energised by sinusoidal excitation with a rated RMS current of 2.56 kA. MV winding i.e., secondary winding loaded by 144.11 Ω and HV winding i.e., tertiary winding loaded by 169.43 Ω . Fig. 10 illustrates the waveform of the sinusoidal current excitation. After simulating, stray losses are calculated by parametric analysis of wall shunt thickness using ANSYS MAXWELL software. In parametric analysis, wall shunt thickness is varied from 4 mm to 40 mm with a step of 2 mm. Stray losses obtained from the parametric analysis is illustrated in Fig. 12.

B) Non-Sinusoidal Excitation

Design of converter transformer remains the same as in the previous case only difference is that LV winding is energised by the non-sinusoidal excitation with a crest value of 3.283 kA. The fundamental component of the non-sinusoidal excitation is given in sinusoidal excitation. So, the crest value of the non-sinusoidal excitation is calculated by equation (2). MV winding i.e. secondary winding loaded by 88.17 Ω and HV winding i.e. tertiary winding loaded by 104.04 Ω . Fig. 11 illustrates the waveform of the non-sinusoidal current excitation. In the parametric analysis of wall shunt thickness, stray losses are analysed after simulating the design in ANSYS MAXWELL shown in Fig. 12.

Fig. 12 shows that the thickness of the wall shunt is increased from 4 mm to 40 mm with a step of 2 mm. It also shows that as the thickness of the wall shunt increased, stray losses are decreased from 127.49 kW to 19.51 kW in sinusoidal excitation and 240.30 kW to 33.66 kW in non-sinusoidal excitation due to vertical wall shunt.

4.2. Horizontal Wall Shunt

In this case, horizontal wall shunt is utilized instead of vertical wall shunt in which wall shunt placed in parallel to yoke of converter transformer as illustrated in Fig. 5.

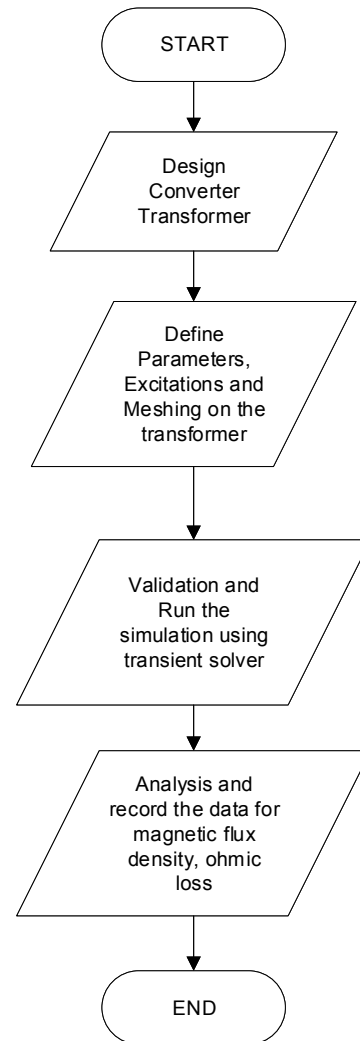


Fig. 7. Flow Chart of The Loss Calculation Using 3D FEA Method

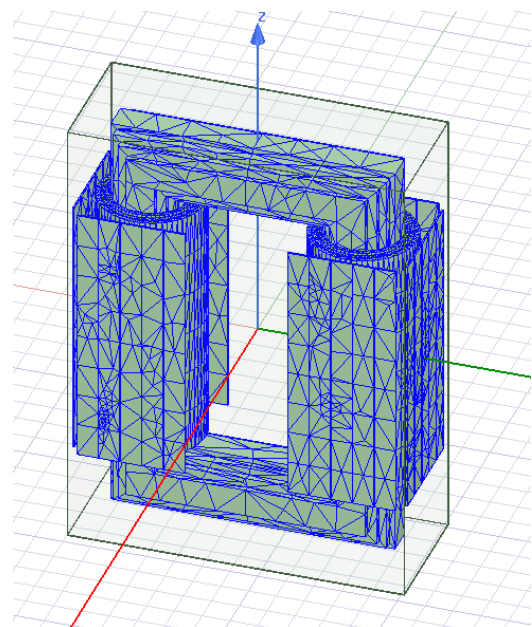


Fig. 8. Meshed Model of Converter Transformer Using Vertical Wall Shunt

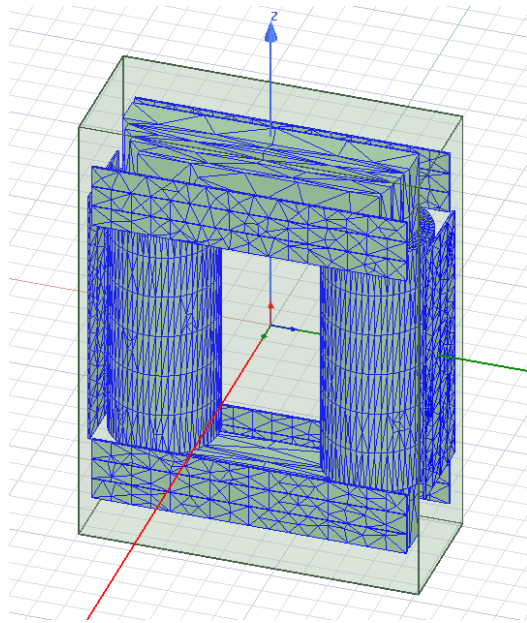


Fig. 9. Meshed Model of Converter Transformer Using Horizontal Wall Shunt

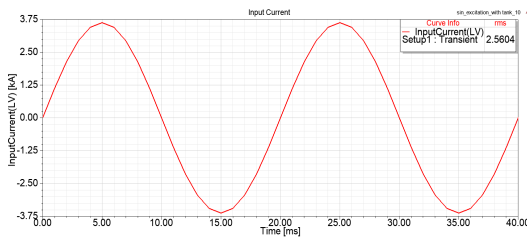


Fig. 10. Sinusoidal Excitation Current Waveform

A) Sinusoidal Excitation

In this section, loading and current excitation parameters are identical to those in the preceding sinusoidal excitation instance with a vertical wall shunt. Fig. 13 shows the stray losses determined from parametric analysis.

B) Non-Sinusoidal Excitation

In this case, loading and current excitation parameters are identical to non-sinusoidal excitation with vertical wall shunt. In the parametric analysis of wall shunt thickness, stray losses are analysed after simulating the design in ANSYS MAXWELL shown in Fig. 13. From Fig. 13, it is seen that as the wall shunt thickness increased from 4mm to 40mm stray losses are decreased from 41.10kW to 18.58kW in sinusoidal excitation and 61.66kW to 24.16kW in non-sinusoidal excitation due to horizontal wall

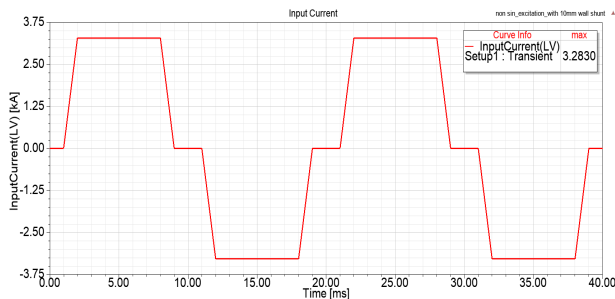


Fig. 11. Non-Sinusoidal Excitation Current Waveform

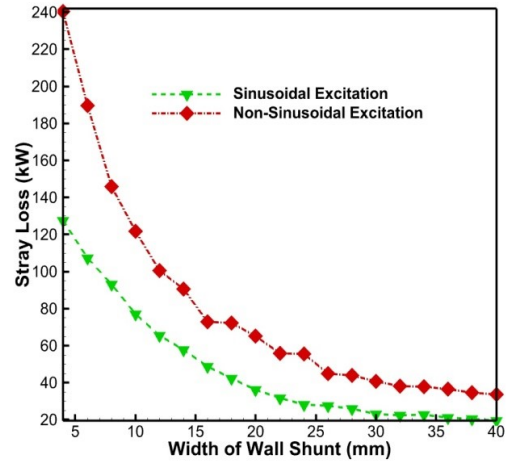


Fig. 12. Parametric Analysis of Vertical Wall Shunt

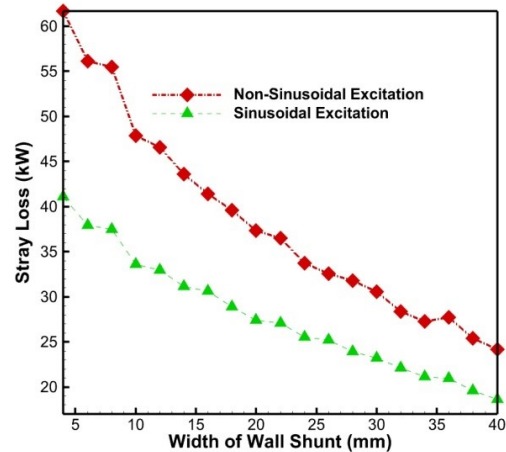


Fig. 13. Parametric Analysis of Horizontal Wall Shunt

shunt.

Fig. 12 and Fig. 13 show that stray losses are less in sinusoidal excitation than non-sinusoidal excitation because non-sinusoidal excitations are fundamental components given to the sinusoidal excitation.

Also, during parametric analysis for the increase in thickness of wall shunt, it is considered that when the thickness of wall shunt increases which reduces the distance between wall shunt and transformer tank as well as the distance between wall shunt and transformer winding which causes increase in faults of the transformer. So, for the optimum location and appropriate thickness of wall shunt FEM method is used. In the designed transformer, the parametric analysis of the graph shows that after a certain thickness of wall shunt decrease in stray loss is very less.

Fig. 14 and Fig. 15 show the magnetic flux density distribution for the 4mm wall shunt of vertical as well as horizontal wall shunt respectively. From Fig. 14 and Fig. 15 seen that if the thickness of wall shunt is less then these wall shunt are saturate at very low magnetic flux density which increases the thermal temperature of the wall shunt and also, these wall shunt cannot effectively reduces the stray losses. Therefore with the increase in thickness of wall shunt stray losses are reduced.

Fig. 16 shows that the magnetic flux density on the vertical wall shunt is not evenly distributed and most of the vertical wall shunt plates have low value of magnetic flux density. Also, the value flux density on the vertical wall shunt's surface is less than the

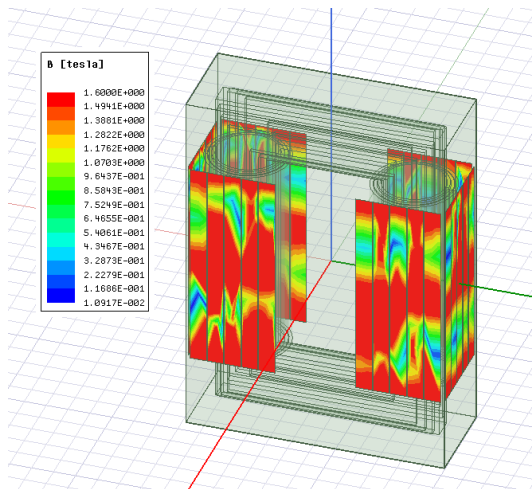


Fig. 14. Distribution of Magnetic Flux Density on 4mm Vertical Wall Shunt

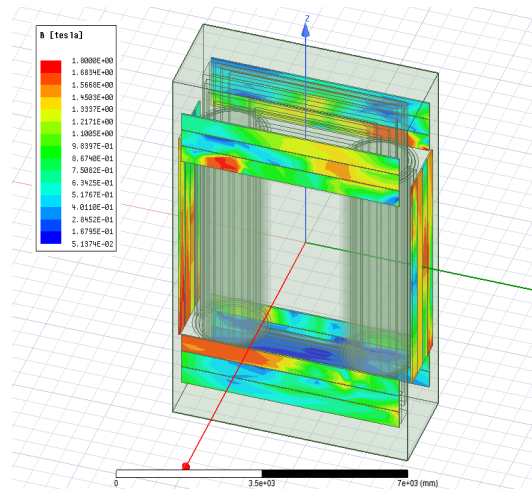


Fig. 17. Distribution of Magnetic Flux Density on 40mm Horizontal Wall Shunt

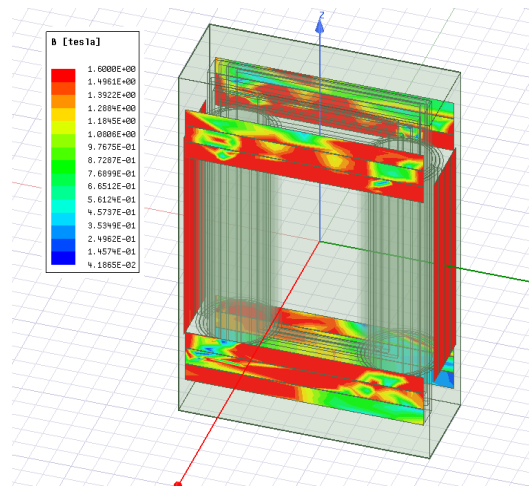


Fig. 15. Distribution of Magnetic Flux Density on 4mm Horizontal Wall Shunt

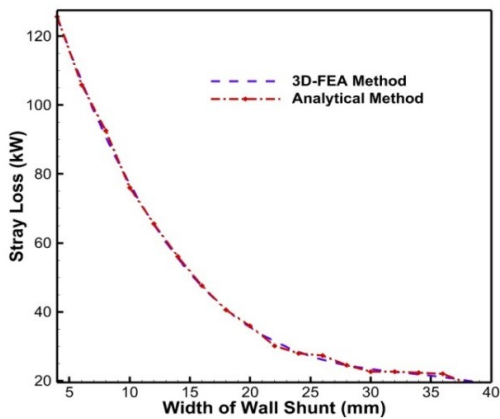


Fig. 18. Parametric Analysis of Vertical Wall Shunt for Sinusoidal Excitation

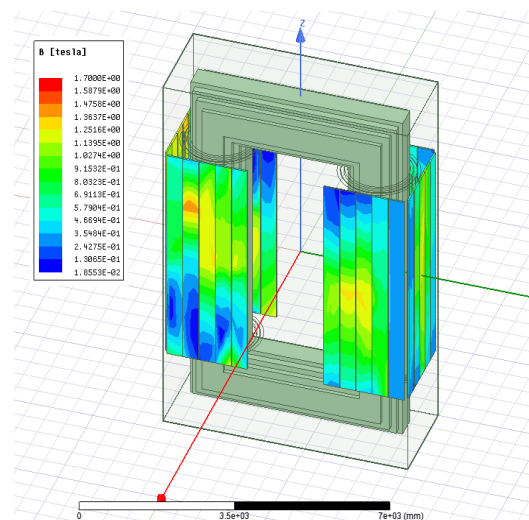


Fig. 16. Distribution of Magnetic Flux Density on 40mm Vertical Wall Shunt

horizontal wall shunt. As a result, the quantity of leakage magnetic fluxes that travel through this vertical wall shunt is less.

The magnetic flux density on the horizontal wall shunt is evenly distributed, as shown in Fig. 17. Also, the value of magnetic flux density shows that the leakage fluxes that travel through the horizontal wall shunt are higher than the earlier case of vertical wall shunt. Fig. 17 also shows that the all horizontal wall shunt plates are effectively used and maximum value of flux density is 1.8T which is passing through the horizontal wall shunt. Saturation point of the M5 material is around 1.8T [35] and the maximum flux density passing through the horizontal wall shunt is 1.8T. So, maximum leakage fluxes will pass through the horizontal wall shunt and these leakage fluxes are not in direct contact with the transformer tank due to this transformer tank stray losses is reduced.

Stray losses evaluated by the 3D FEA method i.e., numerical analysis are also verified using the analytical method. In the analytical method, stray losses are estimated using equation (17). In equation (17), consider the conductivity of medium i.e. transformer tank's material conductivity is 2×10^6 mho/m and $\int_{surface} (H_b)^2 ds$ is evaluated on transformer tanks surface using FEA software's field calculator.

Fig. 18 and Fig. 19 shows that the stray losses obtained from 3D-FEA method are nearly equal to the analytical method in vertical wall shunt for both excitations. Fig. 20 and Fig. 21

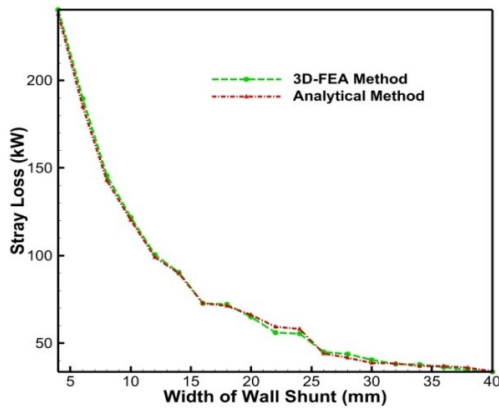


Fig. 19. Parametric Analysis of Vertical Wall Shunt for Non-sinusoidal Excitation

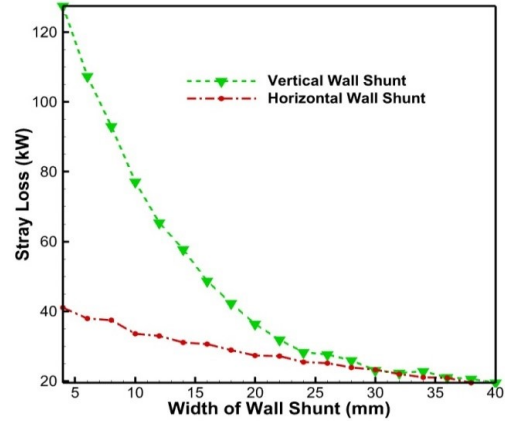


Fig. 22. Parametric Analysis for Sinusoidal Excitation using 3D-FEA Method

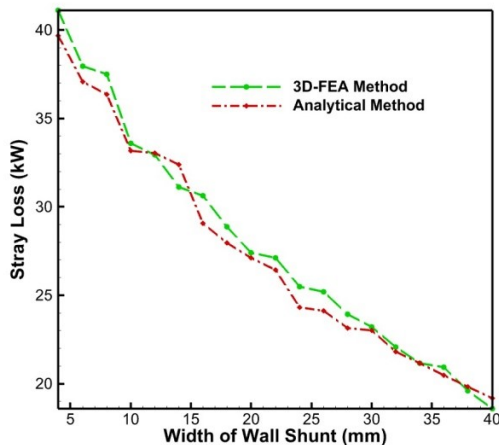


Fig. 20. Parametric Analysis of Horizontal Wall Shunt for Sinusoidal Excitation

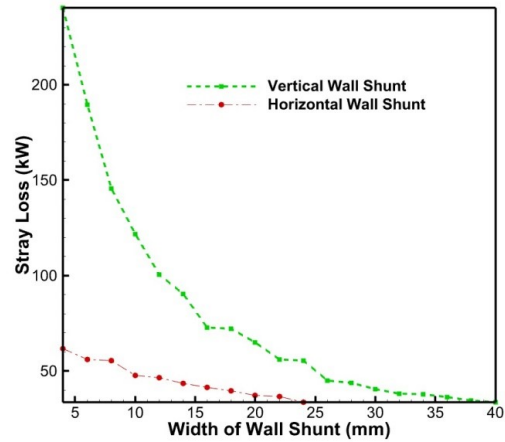


Fig. 23. Parametric Analysis for Non-sinusoidal Excitation using 3D-FEA Method

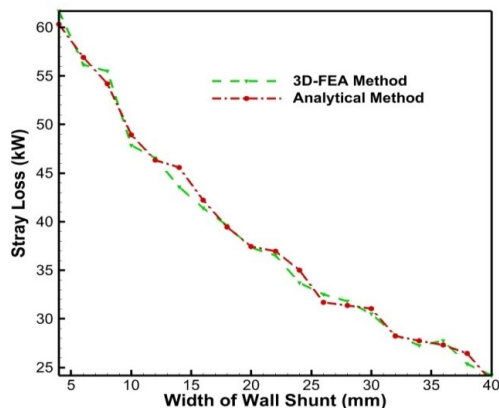


Fig. 21. Parametric Analysis of Horizontal Wall Shunt for Non-sinusoidal Excitation

indicate that the stray losses estimated from the 3D-FEA approach in horizontal wall shunt are almost equal to those obtained from the analytical technique for both excitations. Fig. 22 illustrates that horizontal wall shunt converter transformer has low stray losses compared to the vertical wall shunt for sinusoidal excitation. Fig. 23 shows that the converter transformer with vertical wall shunts have more losses than horizontal wall shunts for non-sinusoidal excitation. Also from the above results it is seen that after certain thickness i.e. 36mm of wall shunt effectiveness of stray losses reduction is reduced as compared to the previous cases i.e. from 4mm to 36mm parametric analysis of wall shunt. From the above results, it is observed that stray losses in the horizontal wall shunt have less stray losses than vertical wall shunt. Horizontal wall shunt requires less number of wall shunt for the reduction of stray losses compared to vertical wall shunt, so the cost and weight of the converter transformer are reduced. Also, horizontal wall shunt effectively reduces stray losses. In the parametric analysis of wall shunt thickness, it is observed that stray losses are reduced with the increase in wall shunt thickness.

5. CONCLUSION

In this paper, ANSYS MAXWELL software is used for designing converter transformer. The current flowing through the converter transformer winding is non-sinusoidal due to the sequence operation of bridges connected to the converter transformer winding. So, the stray losses are more in converter

transformer due to the non-sinusoidal current in the winding. Horizontal wall shunt and vertical wall shunt are used to reduce stray losses applied to the transformer tank. In this paper, stray losses are estimated by parametric analysis of wall shunt thickness for both types of wall shunt using 3D-FEA method. The results show that, in non-sinusoidal excitation, stray losses are more than the fundamental component of non-sinusoidal excitation, i.e. sinusoidal excitation. In parametric analysis of wall shunt for the increase in thickness of wall shunt from 4mm to 40mm, stray losses are decreased from 127.49kW to 19.51kW in sinusoidal excitation and 240.30kW to 33.66kW in non-sinusoidal excitation due to vertical wall shunt as well as for horizontal wall shunt, stray losses are decreased from 41.10kW to 18.58kW in sinusoidal excitation and 61.66kW to 24.16kW in non-sinusoidal excitation. From the above results it is seen that, stray losses are reduced with the increase in wall shunt thickness. Also, horizontal wall shunt reduces stray losses more effectively than vertical wall shunt. The number of wall shunt plates used in horizontal wall shunt is less than vertical wall shunt. So, in horizontal wall shunt converter transformer, the cost and size of converter transformer are reduced. The result which is obtained from 3D-FEA method is compared with the analytical method. This parametric analysis is used to find the location and thickness of wall shunt to reduce stray losses before installation at the site effectively.

REFERENCES

- [1] A. M. Elsayed, A. M. Shaheen, M. M. Alharthi, S. S. Ghoneim, and R. A. El-Sehiemy, "Adequate Operation of Hybrid AC/MT-HVDC Power Systems Using an Improved Multi-Objective Marine Predators Optimizer," *IEEE Access*, vol. 9, pp. 51065–51087, 2021.
- [2] H. Mirzaei, "Investigating the Practical Applications of the Frequency Response of the Transformers Extracted Using the Lightning Impulse Test Results," *J. Oper. Automa. Power Eng.*, vol. 10, pp. 206–213, 2022.
- [3] Z. Moravej and S. Bagheri, "Condition monitoring techniques of power transformers: A review," *J. Oper. Automa. power Eng.*, vol. 3, pp. 71–82, 2015.
- [4] X. Wang, J. Yang, X. Cao, M. Xu, and J. Lv, "The electric tests of ordinate insulation in converter transformer by the method of applying voltage on single-phase," *7th Int. Conf. Properties Applic. Dielectric Materials (Cat. No. 03CH37417)*, pp. 1170–1173, 2003.
- [5] L. F. de Oliveira, N. Sadowski, and S. H. L. Cabral, "Alternative model for computing transformer tank induced losses in the time domain," *IET Electric Power Applica.*, vol. 14, pp. 2507–2514, 2020.
- [6] S. Vasilija, "FEM 2D and 3D design of transformer for core losses computation," *Machines. Technologies. Materials*, 2017, pp. 345–348.
- [7] A. N. Hamoodi, B. A. Hammad, and F. S. Abdullah, "Experimental simulation analysis for single phase transformer tests," *Majlesi J. Electric. Eng.*, vol. 14, pp. 91–95, 2020.
- [8] F. Dughiero and M. Forzan, "Transient magnetic fem analysis for the prediction of electrodynamic forces in transformers with magnetic shunts," *IEEE Int. Magnetics Conf. (INTERMAG)*, p. EV5, 2002.
- [9] M. Mikhak-Beyranvand, J. Faiz, and B. Rezaealam, "Thermal analysis and derating of a power transformer with harmonic loads," *IET Gener. Transm. Distrib.*, vol. 14, pp. 1233–1241, 2020.
- [10] A. Torkaman and V. Naeini, "Recognition and Location of Power Transformer Turn to Turn Fault by Analysis of Winding Imposed Forces," *J. Oper. Autom. Power Eng.*, vol. 7, pp. 227–234, 2019.
- [11] M. Djurovic and J. Monson, "3-dimensional computation of the effect of the horizontal magnetic shunt on transformer leakage fields," *IEEE Trans. Magnetics*, vol. 13, pp. 1137–1139, 1977.
- [12] A. Di Pasquale, G. Antonini, and A. Orlandi, "Shielding effectiveness for a three-phase transformer at various harmonic frequencies," *IET scie. measur. & technology*, vol. 3, pp. 175–183, 2009.
- [13] H. Wang, Q. Yang, Y. Li, J. Wang, and D. Tian, "Numerical Analysis of the Effect of Magnetic Shielding on Stray Losses in Adjacent Parts of Power Transformer Ascending Flange," *IEEE Int. Conf. Applied Superconductivity Electromag. Devi. (ASEMD)*, pp. 1–2, 2020.
- [14] S. J. Arand and K. Abbaszadeh, "The study of magnetic flux shunts effects on the leakage reactance of transformers via FEM," *Majlesi J. Electric. Eng.*, vol. 4, pp. 47–52, 2010.
- [15] V. Behjat, A. Shams, and V. Tamjidi, "Characterization of power transformer electromagnetic forces affected by winding faults," *J. Oper. Autom. Power Eng.*, vol. 6, pp. 40–49, 2018.
- [16] C. Yongbin, Y. Junyou, Y. Hainian, and T. Renyuan, "Study on eddy current losses and shielding measures in large power transformers," *IEEE trans. magnetics*, vol. 30, pp. 3068–3071, 1994.
- [17] M. A. Tsili, A. G. Kladas, P. S. Georgilakis, A. T. Souflaris, and D. G. Paparigas, "Geometry optimization of magnetic shunts in power transformers based on a particular hybrid finite-element boundary-element model and sensitivity analysis," *IEEE trans. magnetics*, vol. 41, pp. 1776–1779, 2005.
- [18] Z. Song, Y. Wang, S. Mou, Z. Wu, Y. Zhu, B. Xiang, et al., "The edge effects of magnetic shunts for a transformer tank," *Int. Conf. Electric. Machines Syst.*, 2011, pp. 1–4.
- [19] A. Sawhney and A. Chakrabarti, "Electrical machine design," *DhanpatRai and Co.*, 2006.
- [20] I. Dasgupta, *Power transformers quality assurance: New Age International*, 2009.
- [21] E. W. Kimbark, *Direct current transmission vol. 1: Wiley*, 1971.
- [22] S. V. Kulkarni and S. Khaparde, *Transformer engineering: design and practice, CRC press*, vol. 25, 2004.
- [23] B. Committee, "Transformers," 2003.
- [24] J. U. Kothavade and P. Kundu, "Investigation Of Electromagnetic Forces In Converter Transformer," *IEEE 2nd Int. Conf. Smart Techno. Power, Energy Contr. (STPEC)*, 2021, pp. 1–6.
- [25] L. Li, W. N. Fu, S. L. Ho, S. Niu, and Y. Li, "Numerical analysis and optimization of lobe-type magnetic shielding in a 334 MVA single-phase auto-transformer," *IEEE Trans. Magnetics*, vol. 50, pp. 1–4, 2014.
- [26] O. Al-Dori, B. Şakar, and A. Dönük, "Comprehensive Analysis of Losses and Leakage Reactance of Distribution Transformers," *Arabian J. Scie. Eng.*, pp. 1–9, 2022.
- [27] C. Hernandez, M. Arjona, and J. Sturgess, "Optimal placement of a wall-tank magnetic shunt in a transformer using FE models and a stochastic-deterministic approach," *12th Biennial IEEE Conf. Electromag. Field Comput.*, pp. 468–468, 2006.
- [28] M. Djurovic and J. Monson, "Stray losses in the step of a transformer yoke with a horizontal magnetic shunt," *IEEE Trans. Power Apparatus Syst.*, pp. 2995–3000, 1982.
- [29] Z. Song, Y. Wang, S. Mou, Z. Wu, Y. Zhu, B. Xiang, et al., "Tank losses and magnetic shunts in a three phase power transformer," *Int. Conf. Elec. Machines Syst.*, 2011, pp. 1–4.
- [30] C. Xiao, C. Dezhi, and B. Baodong, "Study of Loss and Temperature Considering Different Shielding Structure in Power Transformer," *IEEE Int. Magnetic Conf. (INTERMAG)*, pp. 1–5, 2021.
- [31] K.-H. Park, H.-J. Lee, and S.-C. Hahn, "Finite-Element Modeling and Experimental Verification of Stray-Loss Reduction in Power Transformer Tank With Wall Shunt," *IEEE Trans. Magnetics*, vol. 55, pp. 1–4, 2019.
- [32] M. Moghaddami, A. I. Sarwat, and F. De Leon, "Reduction of stray loss in power transformers using horizontal magnetic

- wall shunts," *IEEE Trans. magnetics*, vol. 53, pp. 1–7, 2016.
- [33] L. Susnjic, Z. Haznadar, and Z. Valkovic, "3D finite-element determination of stray losses in power transformer," *Elec. Power Syst. Research*, vol. 78, pp. 1814–1818, 2008.
- [34] N. S. Matthew, *Elements of electromagnetics: Oxford University Press*, 2015.
- [35] S. E. Zirka, Y. I. Moroz, N. Chiesa, R. G. Harrison, and H. K. Høidalen, "Implementation of inverse hysteresis model into EMTP—Part I: Static model," *IEEE Trans. Power Deliv.*, vol. 30, pp. 2224–2232, 2015.